Rigidifying Donor–Acceptor Frameworks via C–C Interlocking to Modulate Excited-State Dynamics in HLCT Emitters

L N S Laya Pagadala,[a] Sivakumar Vaidyanathan,[b] and Mahesh Kumar Ravva*,[a,c]

[a]Department of Chemistry, SRM University-AP, Amaravati-522240, India

[b]Department of Chemistry, Indian Institute of Technology, Hyderabad, Kandi, Sangareddy-502285, India

[c]Centre for Computational and Integrative Sciences, SRM University-AP, Amaravati-522240, India

*Email. mahesh.r@srmap.edu.in

Table S1	Comparative DFT benchmarking results for the experimental molecules a) CzIO and b) CzIP calculated using different exchange-correlation functional with the 6-31G(d,p) as basis set.
Table S2	Calculated dihedral angles of ortho and para substituted molecules from optimized geometries with DFT PBE0/6-31G(d,p) level of theory.
Fig.S1	FMO Analysis are performed to a) ortho and b) para molecules using PBE0/6-31G(d,p) level of theory in gaussian TDDFT.
Table S3	Calculated HOMO and LUMO values are performed under PBE0/6-31g** level of theory in gaussian TDDFT.
Fig.S2	Pictorial representation of NTOs of various a) ortho and b) para substituted molecules in the lowest singlet state (S1) as determined at the TD-PBE0/6-31G (d,p) level of theory.
Fig.S3	Pictorial representation of NTOs of various a) ortho and b) para substituted molecules in the higher-lying triplet states (T_m) as determined at the TD-PBE0/6-31G (d,p) level of theory.
Table S4	Calculated Δr (in Å) indices for the designed ortho and para substituted molecules.
Table S5	Calculated lower singlet and triplet gaps of ortho and para substituted molecules with the PBE0/6-31G(d,p) level of theory.
Table S6	Calculated oscillator strength (f), emission energies (in eV), and radiative rates (k_r in s^{-1}) of ortho and para interlocked molecules.

Table of contents

Table S1. Comparative DFT benchmarking results for the experimental molecules a) CzIO and b) CzIP calculated using different exchange-correlation functional with the 6-31G(d,p) as basis set.
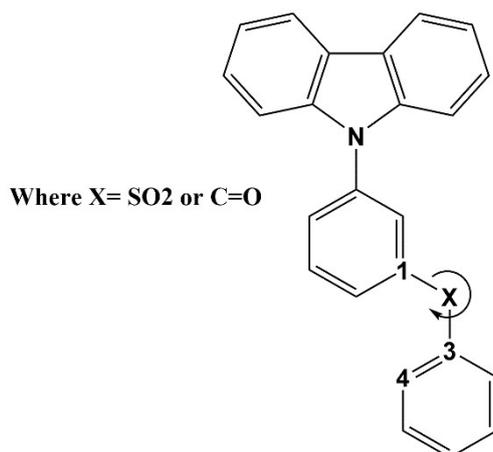
a) **CzIO molecule**

Method	HOMO (eV)	LUMO (eV)	LUMO-HOMO (eV)	S1 (eV)	Absorption nm
B3LYP	-5.94	-2.25	3.68	3.14	395
PBE0	-6.24	-2.21	4.03	3.30	376
BMK	-6.70	-1.64	5.06	3.64	340
M062X	-7.19	-1.42	5.77	3.85	322
CAM-B3LYP	-7.20	-1.07	6.13	3.81	325
wB97XD	-7.82	-0.56	7.26	3.87	320
Experimental[1]	-6.17	-2.16	4.01	3.28	378

b) **CzIP molecule**

Method	HOMO (eV)	LUMO (eV)	LUMO-HOMO (eV)	S1 (eV)	Absorption nm
B3LYP	-5.98	-2.27	3.70	3.26	381
PBE0	-6.27	-2.24	4.04	3.39	365
BMK	-6.73	-1.69	5.04	3.70	335
M062X	-7.22	-1.51	5.72	3.84	323
CAM-B3LYP	-7.23	-1.15	6.08	3.83	324

wB97XD	-7.85	-0.65	7.20	3.88	320
Experimental[1]	**-6.27**	**-2.20**	**4.07**	**3.42**	**363**

Table S2. Calculated dihedral angles of ortho and molecules from ground-state geometries using the PBE0/6-31G(d,p) level of theory.
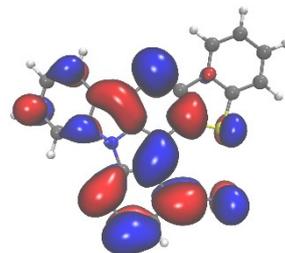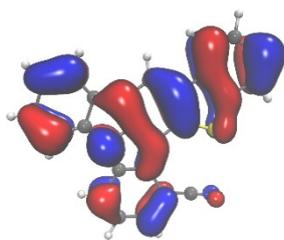

Where X= SO2 or C=O

Molecules	Dihedral angles (^{0})
CzBCNO	0
CzBPO	29
CzBSO	82
CzIO	0
B1CzBCNO	0
B1CzBPO	22
B1CzBSO	91
B1CzIO	0
B2CZBCNO	0
B2CzBPO	22
B2CzBSO	91
B2CzIO	0
CzBCNP	0
CzBPP	31
CzBSP	93
CzIP	0
B1zBCNP	0
B1CzBPP	31
B1CzBSP	87
B1CzIP	0
B2CZBCNP	0
B2CzBPP	31
B2CzBSP	87
B2CzIP	0

a) **FMO of Ortho molecules**

Molecule Name	HOMO	LUMO
CzBCNO		
CzBPO		
CzBSO		
CzIO		

B1CzBCNO

B1CzBPO
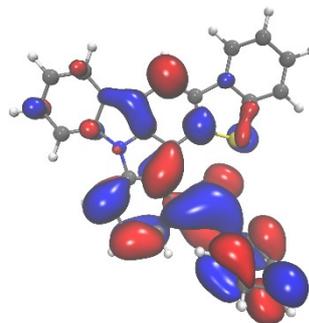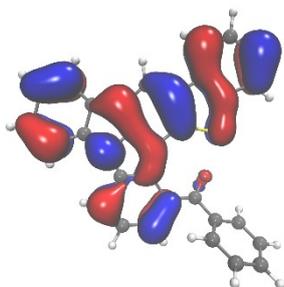
B1CzBSO
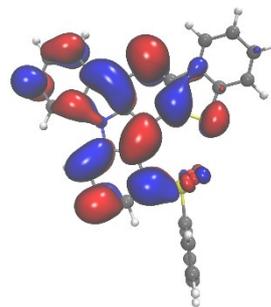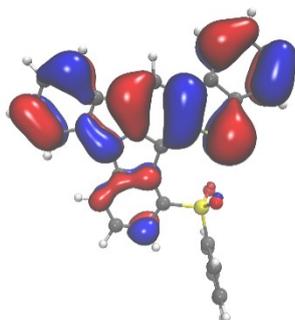
B1CzIO
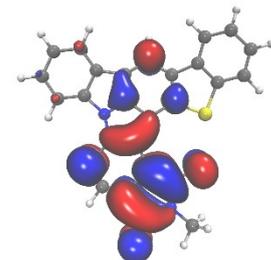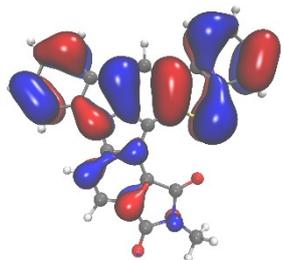
B2CZBCNO
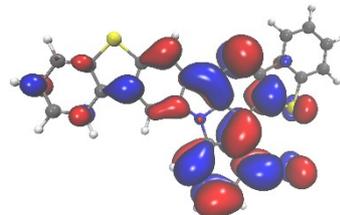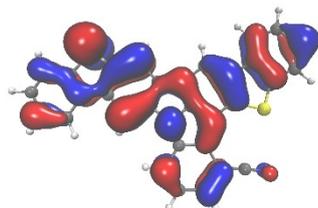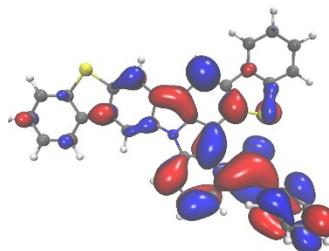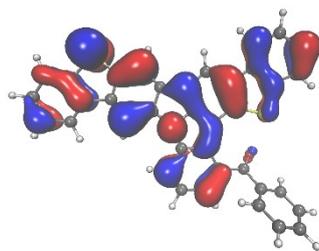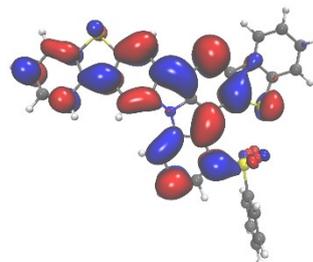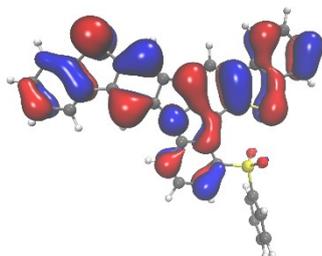
B2CzBPO		
B2CzBSO		
B2CzIO		
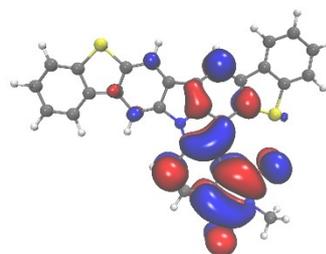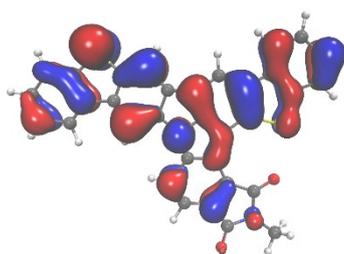
b) FMO of para molecules:

Molecule Name	HOMO	LUMO
CzBCNP		
CzBPP		

CzBSP
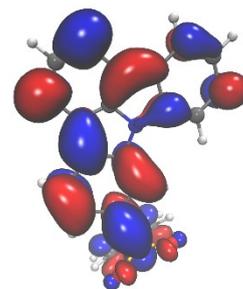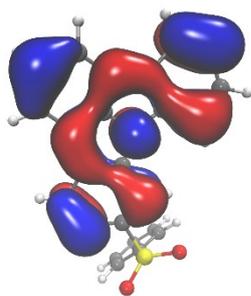
CzIP
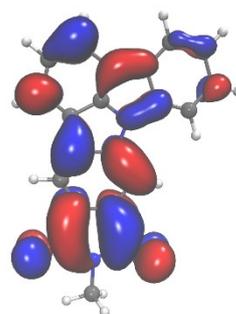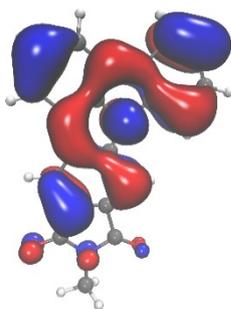
B1CzBCNP

B1CzBPP

B1CzBSP

B1CzIP

B2CZBCNP

B2CzBPP

B2CzBSP
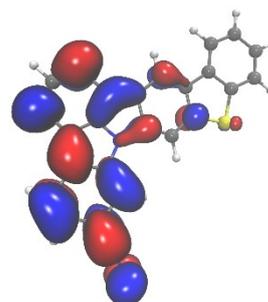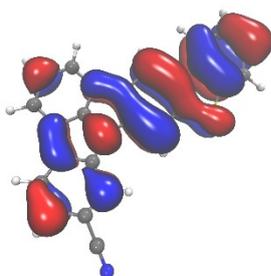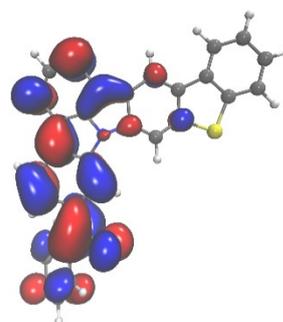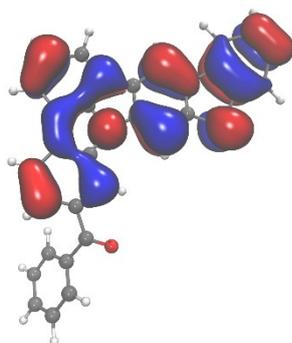
B2CzIP

Fig.S1. FMO Analysis are performed to a) ortho and b) para molecules using PBE0/6-31G(d,p) level of theory in gaussian TDDFT.

Table S3. Calculated HOMO and LUMO values and their gaps are performed under PBE0/6-31G(d,p) level of theory in gaussian TDDFT.

Molecules	HOMO (eV)	LUMO (eV)	ΔEg (eV)
CzBCNO	-6.22	-1.80	4.42
CzBPO	-6.07	-1.93	4.14
CzBSO	-6.17	-1.62	4.55
CzIO	-6.24	-2.18	4.06
B1CzBCNO	-6.06	-1.89	4.17
B1CzBPO	-5.93	-1.90	4.03
B1CzBSO	-5.96	-1.68	4.28
B1CzIO	-6.04	-2.25	3.79
B2CZBCNO	-5.89	-1.98	3.92
B2CzBPO	-5.78	-1.94	3.84
B2CzBSO	-5.83	-1.81	4.02
B2CzIO	-5.89	-2.27	3.62
CzBCNP	-6.22	-1.86	4.36
CzBPP	-6.08	-1.98	4.10
CzBSP	-6.19	-1.79	4.40
CzIP	-6.27	-2.20	4.07
B1CzBCNP	-5.99	-1.88	4.11
B1CzBPP	-5.90	-2.00	3.90
B1CzBSP	-5.97	-1.81	4.16
B1CzIP	-6.03	-2.22	3.81
B2CZBCNP	-5.90	-2.13	3.77
B2CzBPP	-5.80	-2.16	3.64
B2CzBSP	-5.87	-2.06	3.81
B2CzIP	-5.94	-2.24	3.70

a) **Singlet state (S₁) NTOs of ortho molecules:**

Molecule Name	Hole	Electron	Weightage
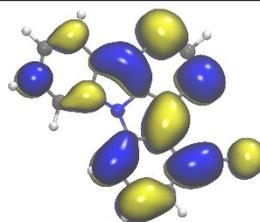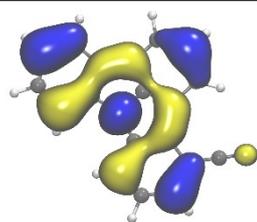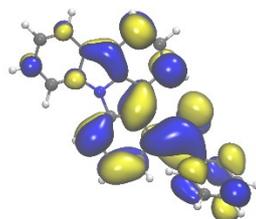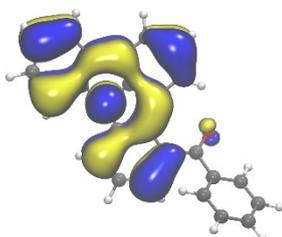
CzBCNO			**97%**
CzBPO			**98%**
CzBSO			**96%**
CzIO			**98%**
B1CzBCNO			**96%**
B1CzBPO			**97%**
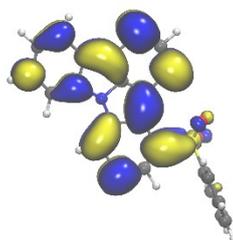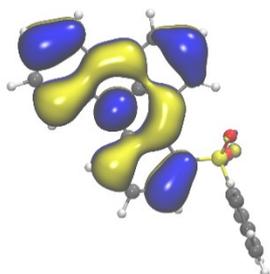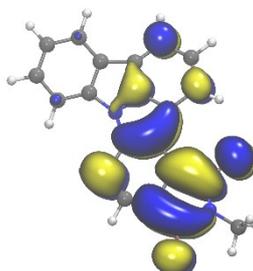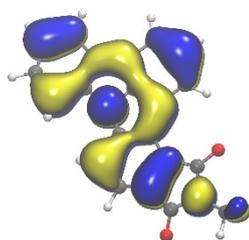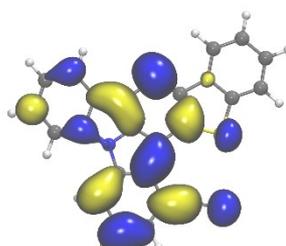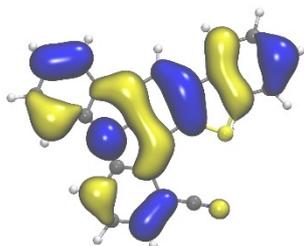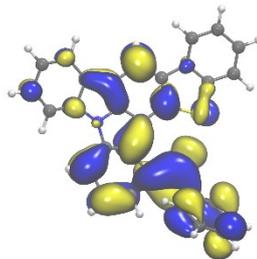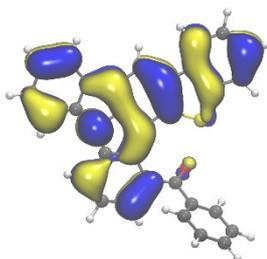
B1CzBSO
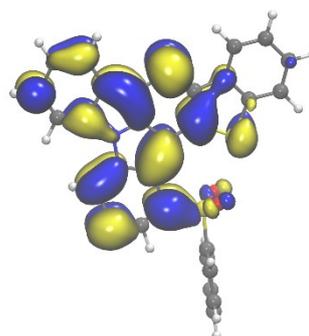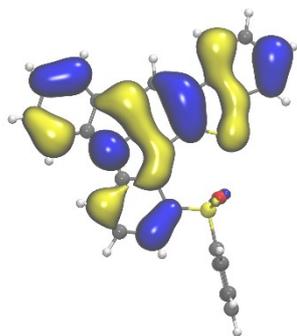
94%

B1CzIO
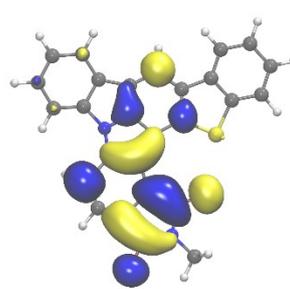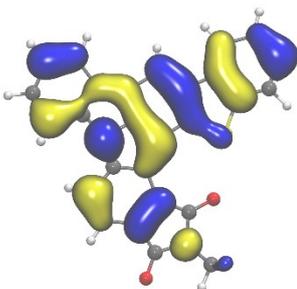
98%

B2CzBCNO
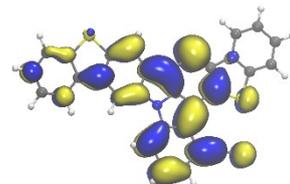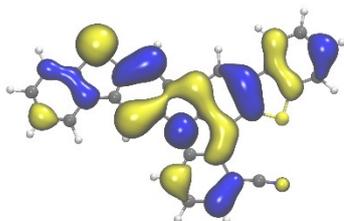
97%

B2CzBPO
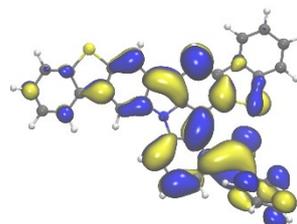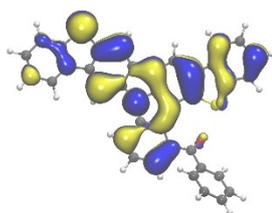
97%

B2CzBSO
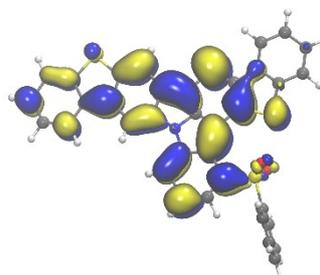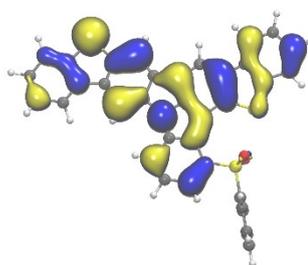
96%
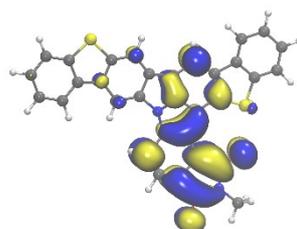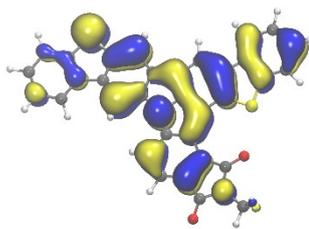
B2CzIO			**98%**

b) Singlet state (S₁) NTOs of para molecules:

Molecule Name	Hole	Electron	Weightage
CzBCNP			**97%**
CzBPP			**97%**
CzBSP			**97%**

CzIP   **97%**

B1CzBCNP   **97%**

B1CzBPP   **98%**

B1CzBSP   **96%**

B1CzIP   **97%**

B2CZBCNP		**97%**
B2CzBPP		**98%**
B2CzBSP		**97%**
B2CzIP		**97%**

Fig.S2: Pictorial representation of NTOs of various a) ortho and b) para substituted molecules in the lowest singlet state (S_1) as determined at the TD-PBE0/6-31G (d,p) level of theory.

electron

57% **42%** **69%** **15%**

hole

CzBCNO, T$_4$ (3.48 eV)   **CzBPO, T$_5$ (3.38 eV)**

electron

59% **41%** **75%** **18%**

hole

CzBSO, T$_5$ (3.65 eV)   **CzIO, T$_4$ (3.25 eV)**

electron

44% **39%** **46%** **30%**

hole

B1CzBCNO, T$_5$ (3.39 eV)   **B1CzBPO, T$_5$ (3.24 eV)**

electron

64% **21%** **52%** **45%**

hole

B1CzBSO, T$_4$ (3.29 eV)   **B1CzIO, T$_3$ (3.03 eV)**

electron

↑ 51% ↑ 31%   ↑ 81% ↑ 18%

hole

B2CzBCNO, T$_4$ (3.19 eV)   **B2CzBPO, T$_5$ (3.18 eV)**

electron

↑ 62% ↑ 18%   ↑ 68% ↑ 28%

hole

B2CzBSO, T$_4$ (3.27 eV)   **B2CzIO, T$_4$ (2.94 eV)**

(a) Ortho

electron

↑ 82% ↑ 11%   ↑ 71% ↑ 13%

hole

CzBCNP, T$_3$ (3.06 eV)   **CzBPP, T$_4$ (3.14 eV)**

electron

↑ 58% ↑ 39%   ↑ 82% ↑ 9%

hole

CzBSP, T$_4$ (3.57 eV)   **CzIP, T$_3$ (2.98 eV)**

S16

electron

hole

B1CzBCNP, T$_4$ (3.24 eV)   **B1CzBPP, T$_5$ (3.22 eV)**

64%   20%   59%   22%

electron

hole

B1CzBSP, T$_4$ (3.29 eV)   **B1CzIP, T$_3$ (2.90 eV)**

64%   18%   92%

electron

hole

B2CzBCNP, T$_3$ (2.79 eV)   **B2CzBPP, T$_3$ (2.84 eV)**

77%   10%   74%   11%

electron

hole

B2CzBSP, T$_3$ (2.91 eV)   **B2CzIP, T$_3$ (2.70 eV)**

69%   14%   73%   14%

(b) Para

Fig.S3: Pictorial representation of NTOs of various a) ortho and b) para substituted molecules in the higher-lying triplet states (T$_m$) as determined at the TD-PBE0/6-31G (d,p) level of theory.

Table S4. Calculated Δr (in Å) indices for S_1 state for the designed ortho and para substituted molecules at the PBE0/6-31G(d,p) level of theory.

Molecules	Δr (in Å)
CzBCNO	1.68
CzBPO	3.13
CzBSO	1.26
CzIO	3.13
B1CzBCNO	2.20
B1CzBPO	2.98
B1CzBSO	1.15
B1CzIO	2.26
B2CzBCNO	2.25
B2CzBPO	2.72
B2CzBSO	0.73
B2CzIO	3.67
CzBCNP	1.40
CzBPP	2.85
CzBSP	1.32
CzIP	2.35
B1CzBCNP	3.38
B1CzBPP	1.67
B1CzBSP	2.51
B1CzIP	3.59
B2CZBCNP	1.68
B2CzBPP	2.20
B2CzBSP	1.36
B2CzIP	4.85

Table S5. Calculated lower singlet and triplet gaps of ortho and para interlocked molecules with the PBE0/6-31G(d,p) level of theory.

Molecules	S_1(eV)	T_1(eV)	T_2(eV)	T_3(eV)	T_4(eV)	T_5(eV)	$\Delta S_1 T_1$(eV)	$\Delta S_1 T_2$(eV)	$\Delta S_1 T_3$(eV)	$\Delta S_1 T_4$(eV)	$\Delta S_1 T_5$(eV)
CzBCNO	3.61	2.80	2.94	3.24	3.48	3.83	0.81	0.67	0.38	0.13	-0.22
CzBPO	3.41	2.76	2.88	3.05	3.18	3.38	0.65	0.53	0.36	0.23	0.03
CzBSO	3.71	2.86	3.08	3.27	3.58	3.65	0.85	0.63	0.44	0.13	0.06
CzIO	3.27	2.66	2.85	3.20	3.25	3.48	0.61	0.42	0.07	0.02	-0.21
B1CzBCNO	3.42	2.58	2.83	3.21	3.23	3.39	0.84	0.59	0.22	0.20	0.03
B1CzBPO	3.33	2.63	2.87	3.08	3.20	3.24	0.70	0.46	0.25	0.13	0.09
B1CzBSO	3.54	2.66	2.95	3.26	3.29	3.59	0.88	0.59	0.28	0.25	-0.05

B1CzIO	3.07	2.50	2.67	3.03	3.08	3.23	0.57	0.40	0.04	-0.01	-0.16
B2CZBCNO	3.22	2.51	2.69	2.96	3.19	3.27	0.71	0.53	0.26	0.02	-0.06
B2CzBPO	3.18	2.54	2.72	2.96	3.07	3.18	0.64	0.46	0.22	0.11	0.00
B2CzBSO	3.31	2.54	2.81	3.00	3.27	3.33	0.77	0.50	0.31	0.04	-0.02
B2CzIO	2.95	2.46	2.53	2.92	2.94	3.11	0.49	0.42	0.03	0.01	-0.16
CzBCNP	3.56	2.78	3.01	3.06	3.77	3.86	0.79	0.55	0.50	-0.20	-0.29
CzBPP	3.36	2.72	2.90	3.01	3.14	3.41	0.63	0.46	0.35	0.21	-0.05
CzBSP	3.61	2.85	3.08	3.13	3.57	3.79	0.76	0.53	0.48	0.05	-0.18
CzIP	3.35	2.68	2.87	2.98	3.54	3.62	0.67	0.48	0.37	-0.19	-0.27
B1CzBCNP	3.40	2.71	2.88	2.97	3.24	3.49	0.69	0.51	0.43	0.15	-0.10
B1CzBPP	3.23	2.69	2.80	2.89	3.11	3.22	0.54	0.43	0.34	0.12	0.01
B1CzBSP	3.45	2.74	2.96	3.03	3.29	3.50	0.71	0.49	0.42	0.16	-0.05
B1CzIP	3.18	2.64	2.73	2.90	3.19	3.36	0.54	0.45	0.28	-0.01	-0.18
B2CZBCNP	2.90	2.28	2.36	2.79	3.03	3.22	0.62	0.54	0.11	-0.13	-0.32
B2CzBPP	3.00	2.44	2.52	2.84	3.05	3.35	0.56	0.48	0.16	-0.05	-0.35
B2CzBSP	3.14	2.47	2.63	2.91	3.15	3.39	0.67	0.51	0.23	-0.01	-0.25
B2CzIP	3.00	2.42	2.56	2.70	3.11	3.24	0.58	0.44	0.30	-0.11	-0.24

Table S6. Calculated oscillator strength (f), emission energies (in eV), and radiative rates (k_r in s^{-1}) of ortho and para interlocked molecules.

Molecules	Oscillator strength (f)	Emission Energies (eV)	k_r (s^{-1})
CzBCNO	0.069	3.30	3.24×10^7
CzBPO	0.168	3.03	6.70×10^7
CzBSO	0.075	3.38	3.72×10^7
CzIO	0.015	2.77	4.92×10^6
B1CzBCNO	0.215	3.10	8.97×10^7
B1CzBPO	0.068	2.57	1.94×10^7
B1CzBSO	0.321	3.20	1.43×10^8
B1CzIO	0.013	2.48	3.47×10^6
B2CzBCNO	0.154	3.01	6.07×10^7
B2CzBPO	0.197	2.70	6.23×10^7
B2CzBSO	0.800	3.07	3.27×10^8

B2CzIO	0.011	2.44	2.84×10^6
CzBCNP	0.097	3.22	4.36×10^7
CzBPP	0.104	3.02	4.12×10^7
CzBSP	0.092	3.25	4.22×10^7
CzIP	0.188	2.92	6.96×10^7
B1CzBCNP	0.150	3.02	5.94×10^7
B1CzBPP	0.116	2.83	4.03×10^7
B1CzBSP	0.146	3.05	5.89×10^7
B1CzIP	0.316	2.71	1.01×10^8
B2CzBCNP	0.412	2.86	1.46×10^8
B2CzBPP	0.307	2.72	9.86×10^7
B2CzBSP	0.412	2.89	1.49×10^8
B2CzIP	0.227	2.65	1.35×10^8

6. MD Simulations

For MD simulations, the well-known OPLS-AA (all-atom optimized potentials for liquid simulations) force field for organic molecules was used. The restrained electrostatic potential (RESP) fitting method was used to calculate the partial charges for the molecules. 100 molecules are randomly dispersed in 7 nm*7 nm*7 nm simulation box with periodic boundary conditions (PBC) to generate an initial packing model. The molecules were then compressed for 5 ns at 600 K and 100 bar to bring them closer together. To equilibrate the system, the isothermal-isobaric ensemble MD, also known as NPT-MD, was used. Furthermore, another ten ns simulation was performed at 600 K and 1 bar, then gradually cooling down from 600 K to 300 K within 3 ns. Finally, a 20-ns MD equilibration simulation at 300 K and 1 bar was performed. A Berendsen barostat and a velocity rescaling (V-rescale) thermostat are used to control the pressure and temperature during equilibration. The LINCS algorithm was used to constrain the covalent bonds with hydrogen atoms. A spherical cut-off of 1.2 nm was set for non-bonded short-range interactions (van der Waals and electrostatic interactions). The particle-mesh Ewald (PME) method was employed for long-range interactions. All molecular dynamics simulations were carried out using GROMACS simulations package[1,2]. To assess the impact of molecular rigidity on excited-state properties, we randomly extracted 100 representative conformers of both rigid and non-rigid B2CzBSO molecules from their respective molecular dynamics (MD) trajectories. Time-dependent density functional theory (TD-DFT) calculations were subsequently performed on each conformer to evaluate the energy of the first singlet excited state (S_1).

Reference:

(1) Kuila, S.; Miranda-Salinas, H.; Eng, J.; Li, C.; Bryce, M. R.; Penfold, T. J.; Monkman, A. P. Rigid and Planar π-Conjugated Molecules Leading to Long-Lived Intramolecular Charge-Transfer States Exhibiting Thermally Activated Delayed Fluorescence. *Nat Commun* **2024**, *15* (1), 9611. https://doi.org/10.1038/s41467-024-53740-1.

(2) Woods, R. J.; Chappelle, R. Restrained Electrostatic Potential Atomic Partial Charges for Condensed-Phase Simulations of Carbohydrates. *Journal of Molecular Structure: THEOCHEM* **2000**, *527* (1), 149–156. https://doi.org/10.1016/S0166-1280(00)00487-5.

(3) Abraham, M. J.; Murtola, T.; Schulz, R.; Páll, S.; Smith, J. C.; Hess, B.; Lindahl, E. GROMACS: High Performance Molecular Simulations through Multi-Level Parallelism from Laptops to Supercomputers. *SoftwareX* **2015**, *1–2*, 19–25. https://doi.org/10.1016/j.softx.2015.06.001.